RAPID COMMUNICATIONS

PHYSICAL REVIEW B VOLUME 52, NUMBER 20 15 NOVEMBER 1995-II

Superstructures and defect structures revealed by atomic-scale STM imaging of $WO_3(001)$

F. H. Jones, K. Rawlings, J. S. Foord, P. A. Cox, and R. G. Egdell
New Chemistry Laboratory, South Parks Road, Oxford OX1 2QR, United Kingdom

J. B. Pethica
Department of Materials, Parks Road, Oxford OX1 3PH, United Kingdom

B. M. R. Wanklyn
Clarendon Laboratory, Parks Road, Oxford OX1 3PU, United Kingdom

(Received 13 July 1995)

Atomic-scale images of the (001) surface of monoclinic WO_3 have been obtained by scanning tunneling microscopy. Termination of the surface WO_2 plane with half a monolayer of oxygen ions gives a surface periodicity $\sqrt{2}$ times that of the underlying ReO_3-like framework. An additional periodicity is introduced by tilting of WO_6 octahedra to produce alternately long and short O-O separations along the [110] direction. This produces a (2×2) superstructure approximating the space group $c2mm$. Prominent defect lines at the surface are attributed to missing oxygen ions.

Tungsten trioxide (WO_3) is an important $5d^0$ transition-metal oxide that finds application in a number of technologically important devices including thin-film electrochromic displays[1] and H_2S gas sensors.[2] The material undergoes at least five phase changes at temperatures between 100 and 1000 K.[3] These are associated with tilting and distortion of a framework of corner-sharing WO_6 octahedra to give structures with lower symmetry than the parent cubic structure of ReO_3. The room-temperature monoclinic structure belongs to the space group $P2_1/n$ with cell parameters $a=7.297$ Å, $b=7.539$ Å, $c=7.688$ Å, and $\beta=90.91°$. This represents a $2\times2\times2$ superstructure on an idealized cubic unit cell of dimension ~3.7 Å. A projection of this structure onto the (001) plane is shown in Fig. 1.[4] The band gap of monoclinic WO_3 is about 2.6 eV at 300 K. However, the bulk solid-state properties of WO_3 are dominated by the propensity of the material to become oxygen deficient with variable composition parameter x in WO_{3-x}. For oxygen vacancy concentrations in excess of $x=10^{-4}$, point defects are eliminated to generate well-defined shear planes running along $\langle 1m0\rangle$ directions. These involve edge-sharing WO_6 octahedra.[5]

Little is known about the surface structure of WO_3, beyond the observation of low-energy electron diffraction (LEED) patterns expected for the (001) surface of a perovskitelike material: splitting of the LEED spots arises from microscopic twinning of monoclinic domains.[6] However, there is little prospect of using LEED to probe the nature of defects on WO_3 surfaces: the surface defect structure is of particular interest in view of the cooperative effects manifest in the bulk defect chemistry. In the present paper, we apply scanning tunneling microscopy (STM) to characterize both regular terrace and defect structures on $WO_3(001)$ surfaces. The terrace structure is dominated by the need to terminate the surface without a repeating dipole unit. However, additional doubling of the periodicity along the [110] direction appears to reflect the underlying tilt of the WO_6 octahedra. Thus, distortion of a perovskitelike material has been observed in real space. Surfaces also display well-defined defect troughs running roughly along $\langle 100\rangle$ directions. These involve a cooperative elimination of oxygen ions in the $O_{0.5}$ overlayer that completes the sixfold coordination of half the tungsten ions in the WO_2 surface layer. A particular strength of STM is that it is able to provide both topographic and spectroscopic information, and this aspect of the technique is exploited in the present work to characterize the local electronic structure associated with the defect troughs.

WO_3 crystals were grown by crystallization from a flux. A crystal fragment of approximate dimensions 4 mm$\times$3 mm $\times$3 mm was cleaved in air with a sharp blade to give an optically smooth surface which transpired from LEED to have (001) orientation. Experiments were carried out in an ion and turbomolecular pumped UHV system (base pressure 8×10^{-11} mbar) equipped with an OMICRON STM microscope stage, OMICRON rear-view LEED optics, and

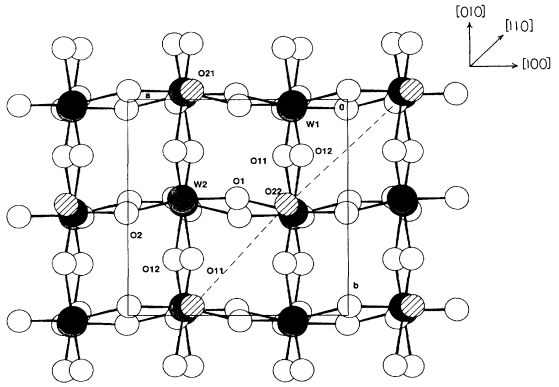

FIG. 1. Projection of the structure of monoclinic WO_3 onto the (001) plane. The surface is terminated with O ions (identified by hatching in the figure) above half the tungsten ions to give a $(\sqrt{2}\times\sqrt{2})R45°$ superstructure based on the primitive ReO_3-like cell. The dashed lines are added to emphasize alternately long and short O-O separations along the [110] direction.

OMICRON cylindical sector analyzer (CSA) analyzer and twin anode x-ray source for x-ray photoemission spectroscopy measurements. The sample was mounted on a Mo plate and held in position with 0.25-mm-diam Ta wire spot welded to the sample plate. The crystal surface was cleaned by annealing in 10^{-5} mbar of oxygen at 650 °C for periods typically of the order of 15 h, heating being effected by radiative emission from a tungsten filament immediately behind the crystal plate. A Chromel-Alumel thermocouple measured the temperature of the sample support plate. Microscope tips were prepared from polycrystalline tungsten wire, as described previously.[7] Tips were degassed by heating at 600 °C before use. The piezodrives in the microscope were calibrated from atomically resolved STM images of Si(111) (7×7) and Ni(110) (1×1).

The cleaning procedure gave rise to surfaces with XPS free of signals due to carbon or other contamination. The W $4f$ core-level signal was a spin-orbit doublet associated with $5d^0$ W(VI) ions: lower binding-energy structure due to reduced W(V) ions was not clearly resolved although the peaks were somewhat broader than expected, possibly due to a small degree of surface reduction. The LEED patterns were found to have twofold symmetry with strong spots at $(\frac{1}{2},\frac{1}{2})$ and $(\frac{1}{2},0)$ but only weak intensity at $(0,\frac{1}{2})$, the superstructures here being defined in relation to an idealized ReO_3-like unit cell of dimensions ~3.7 Å. Splitting of spots along the [100] direction was observed, as in previous work.[6] The spot splitting was independent of beam energy and is attributed to twinning of monoclinic domains along the [010] direction to produce a "zigzag" surface with the surface planes in adjacent domains tilted relative to each other by about 1.8° (i.e., twice the deviation of the monoclinic angle from 90°). In addition, there was evidence for the existence of twin boundaries at which the a and b directions were interchanged: the 90° rotated domains display spot splitting in a direction orthogonal to the unrotated domains. It was possible in LEED to select areas of the crystal surface in which the spot splitting was only along one direction, but many LEED patterns also contained evidence of both 90° rotated domains. The existence of rotated domains means that there is some ambiguity in distinguishing between [100] and [010] directions when interpreting the STM images.

After modest annealing, surfaces displayed large areas of flat terraces in STM. Atomic-scale imaging was most easily achieved at high positive sample bias (typically +1.5 V or +2.0 V). This accords with the fact that slightly nonstoichiometric WO_3 is an n-type semiconductor whose Fermi energy is pinned close to the bottom of the conduction band by donor states associated with oxygen deficiency.[3] Thus tunneling into essentially empty conduction-band states is favored over tunneling from the small number of available donor levels. Over 300 atomically resolved images were acquired over a period of several weeks and in the present paper we concentrate on only two images containing topographic features consistently observed in the majority of the images.

Figure 2 shows a large area image acquired at +1.5 V sample bias and a 1-nA tunnel current. Large terrace areas contain an essentially square array of topographic maxima running along ⟨110⟩ directions. The periodicity of ~5.4 Å revealed by corrugation profiles taken along the [110] topographic rows represents a $\sqrt{2}$ superstructure on the

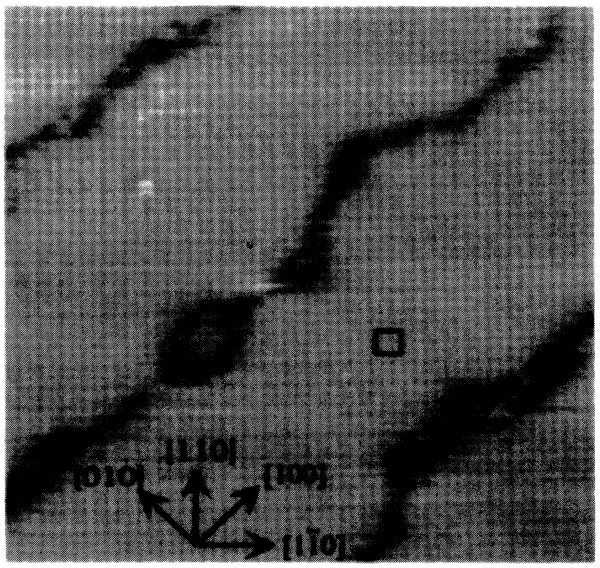

FIG. 2. 150 Å×150 Å image of WO_3(001) acquired at +1.5 V sample bias and a 1-nA tunnel current. The gray scale extends over 4.7 Å. The corrugation along the atomic rows in the [100] direction is 0.3 Å, while the dark troughs have a depth of 1.7 Å. The idealized $(\sqrt{2}\times\sqrt{2})R45°$ unit cell is shown in the figure.

idealized cubic ReO_3 cell rotated by 45°. The origin of this superstructure may be understood by consideration of formal charges on the ionic planes of WO_3. Viewed perpendicular to the (001) plane, the structure is based on a sequence of planes with stoichiometry {O}-{WO_2}-{O}-{WO_2}-{O} carrying formal ionic charges $\{2^-\}$-$\{2^+\}$-$\{2^-\}$-$\{2^+\}$-$\{2^-\}$. A repeating dipolar sequence ($\{2^-\}$-$\{2^+\}$)-($\{2^-\}$-$\{2^+\}$) or ($\{2^+\}$-$\{2^-\}$-($\{2^+\}$-$\{2^-\}$) normal to a surface gives rise to an infinite surface energy,[8] precluding termination of the WO_3 surface in either an {O} or {WO_2} surface plane. However, if a WO_2 plane is covered with a half-monolayer of oxygen, the sequence {$O_{0.5}$}-{WO_2}-{O}-{WO_2}-{O} gives rise to a sequence of ionic charges $\{1^-\}$-$\{2^+\}$-$\{2^-\}$-$\{2^+\}$-$\{2^-\}$ which can be bracketed into the overlapping quadrupolar sequence ($\{1^-\}$-$\{2^+\}$-$\{1^-\}$)-($\{1^-\}$-$\{2^+\}$-$\{1^-\}$): here the $\{2^-\}$ charge of the subsurface {O} layers has been split between two quadrupolar units. This sequence avoids a divergent surface energy. Thus we envisage that half of the surface tungsten ions carry an on-top oxygen ion, these ions being arranged in what is basically a $(\sqrt{2}\times\sqrt{2})R45°$ superstructure.

The topographic maxima are associated with the on-top oxygen ions which sit about 1.9 Å above the W ions of the WO_2 plane. It is often assumed that empty-state STM images of d^0 n-type transition-metal oxides are dominated by cation positions since the conduction-band states probed with positive sample bias are of dominant cation character.[9] However, although the conduction-band states in WO_3 are indeed of dominant W $5d$ atomic character, there is significant mixing with O $2p$ states. The mixing becomes stronger the higher the energy above the bottom of the conduction band. Thus, from the band calculations of Bullett on monoclinic WO_3 we estimate a O $2p$/W $5d$ ratio of 0.17 for states 1.5 eV above the bottom of the conduction band.[10] Ratios of this order will

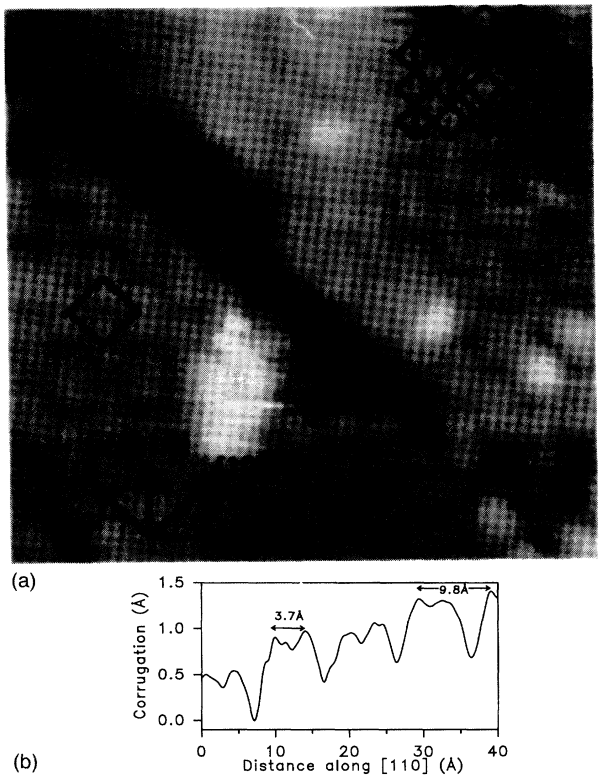

FIG. 3. (a) Higher resolution 78 Å×78 Å image of WO_3(001) acquired at +2.0 V sample bias and a 1-nA tunnel current. The gray scale extends over 5 Å. Note "dimerization" of topographic maxima along the [110] direction. The 2×2 supercell is highlighted in the figure and a schematic representation of the image is shown in the top right-hand corner of the figure. (b) Corrugation profile along the [110] direction. The periodicity of 9.8 Å along this direction introduced by dimerization of the topographic maxima corresponds roughly to $2\sqrt{2}\times 3.7$ Å=10.5 Å within the error limits of the piezo calibration. Dimerization of topographic maxima is apparent.

reduce the apparent topographic height difference between the on-top oxygen ions and the five coordinate W ions in the WO_2 plane, but not by the full distance of order 1.9 Å that represents the W-O distance in the bulk of WO_3: topography continues to dominate density-of-states differences. To put this assertion on a quantitative footing, we use a simple expression for the variation of tunneling current with distance (in Å) of the form[11]

$$I = D\ \exp\{-1.025 d\sqrt{\phi}\},$$

where D is a constant depending on the contribution of an atom to the empty states involved in tunneling and ϕ is the barrier height in eV. Assuming a local barrier height of 2 eV,[12] the density-of-states ratio of 0.17 corresponds to a reduction in the apparent topographic height difference between O and W of only 1.2 Å. Thus, despite band-structure effects it is easy to understand why the protruding oxygen ions correspond to the topographic maxima. Of course, the measured corrugation of 0.3 Å along the rows of topographic maxima is not simply equal to the difference between the W-O bond length (1.9 Å) and the density-of-states factor (1.2 Å): measured corrugations are influenced by a number of additional factors including the effects of finite-tip size, decay of corrugation with increasing surface tip distance,[11] and variations in local barrier height.[13]

High-resolution images of selected smaller areas of the crystal surface as in Fig. 3 (taken at +2.0 V bias) reveal an additional doubling of the periodicity along the [110] direction. This is produced by a "dimerization" of the topographic maxima to produce alternately along and short O-O separations along the [110] direction. The dimerization is most obvious in the corrugation profile taken from the image of Fig. 3. A schematic representation of the STM image is shown as an inset to Fig. 3, which shows that referred to an idealized cubic framework the overall reconstruction is (2×2) and the idealized surface structure belongs to the space group $c2mm$. The origin of the alternation along the [110] direction may be understood in part by reference to the unrelaxed surface terminated bulk crystal structure (Fig. 1). Here it is found that owing to the octahedral tilting and distortion, the separation between adjacent on-top oxygen ions alternates markedly along the [110] with a ratio between long and short distances of 0.45/0.55: there is a much smaller alternation along the [110] direction with long to short ratio of 0.48/0.52. The alternation in STM is actually more pro-

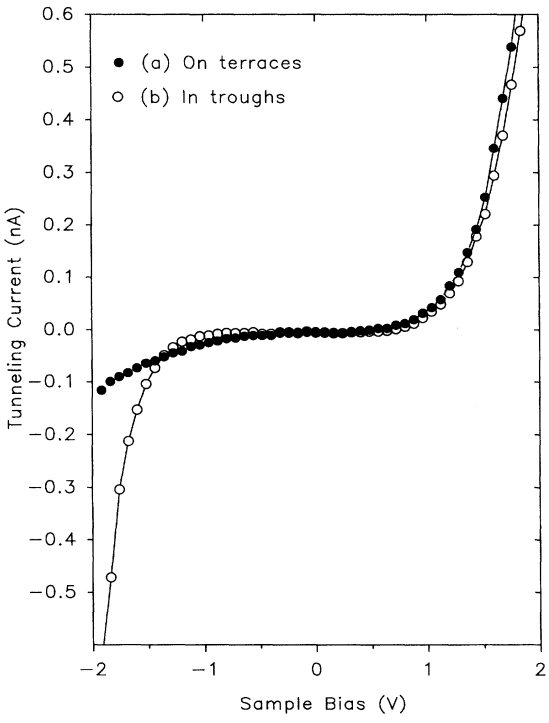

FIG. 4. Current-voltage (I-V) curves for WO_3(001). These were acquired by scanning an STM image at +2.0 V sample bias and a 1-nA tunneling current, with disengagement of the feedback loop at each image point to allow measurement of an I-V curve. The plotted data points correspond to averages of ten image points (a) on terraces and (b) in troughs. Although sufficient topographic resolution was maintained in this mode of scanning to distinguish between terraces and troughs, more detailed topography was not resolved on the terraces.

nounced than in both these cases with a ratio between separations of topographic maxima of 0.38/0.62. This suggests that if the "tilted octahedra" interpretation is correct, the tilting is more pronounced at the surface than in the bulk of the material.

We turn finally to the line defects. These run roughly along [100] and [010] directions, i.e., the directions of the monoclinic twin boundaries. However, we find no evidence of tilting of terraces about the defect lines, so they cannot represent the [010] twin boundaries. The topographic depth of the defect troughs is typically of order 1.7 Å, corresponding roughly to the W-O bond length. Moreover, topographically resolved I-V curves show that whereas on regular terrace sites it is only possible to achieve tunneling into empty states, in the defect troughs there is tunneling from filled states at biases above 1 eV (Fig. 4). We thus associate the defect troughs with areas of the crystal surface where the $O_{0.5}$ on-top oxygen is missing; i.e., termination is in a bare WO_2 plane. Electrical neutrality is maintained if all the underlying W ions of the WO_2 layer are reduced from W(VI) to W(V) to give ions with a localized $5d^1$ electron configuration. Localized electron states may be observed in photoemission from oxygen-deficient WO_3 surfaces at binding energies above about 1 eV.[14,15] The cooperative elimination of on-top oxygen from areas of the crystal surface finds parallels in the cooperative elimination of bulk oxygen to give the crystallographic shear planes: in fact, our topographic troughs run roughly along the directions in which the high-order $(1m0)$ shear planes [i.e., those where m is large and $(1m0)$ approximates (010)] will intersect the (001) surface. However, the idealized (010) shear plane is only $2.5a = 9.3$ Å "wide," whereas the topographic troughs typically have a width of order 20 Å, so they do not represent the simple intersection of bulk shear planes with the surface. In addition, bulk shear plane defects run strictly along well-defined crystallographic directions, whereas the surface troughs meander somewhat in direction.

It remains to be considered why the troughs have an apparent topographic depth of close to the W-O bond length. The large width of the defect troughs allows even a nonideal STM tip to probe the full depth of troughs. However, we have argued earlier that density-of-states differences between W and O should reduce the apparent topographic height difference between on-top O and W ions in the WO_2 plane by something of the order of 1 Å, so that one would not expect to see the bottoms of the troughs 2 Å below the on-top O ions. However, as required by simple considerations of charge balance and as confirmed by spectroscopic I-V measurements, electrons are trapped on the W ions in the trough bottoms. These electrons are expected to exert a Coulomb repulsion on affinity states, which will push the local empty density of states up in energy and reduce the tunneling current at positive sample bias. We therefore propose that a local perturbation of band structure due to electron trapping acts to restore the apparent topographic height difference between on-top O ions and W ions in trough bottoms to a value which accidentally comes close to the bulk W-O bond length.

This work was supported by EPSRC Grant No. GRH/64842.

[1] S. K. Deb, Philos. Mag. **27**, 801 (1973).

[2] M. J. Madou and S. R. Morrison, *Chemical Sensing With Solid State Devices* (Academic, London, 1989).

[3] A. Hamnett and J. B. Goodenough, in *Semiconductors*, edited by O. Madelung, Landolt-Bornstein, New Series, Group III, Vol. 17, Pt. g (Springer-Verlag, Berlin, 1984).

[4] B. O. Loopstra and P. Boldrini, Acta Crystallogr. **21**, 158 (1966).

[5] K. Kosuge, *Chemistry of Non-Stoichiometric Compounds* (Oxford University Press, Oxford, 1994).

[6] M. A. Langell and S. Bernasek, J. Vac. Sci. Technol. **17**, 1296 (1980).

[7] J. P. Ibe, P. P. Bey, Jr., S. L. Brandow, R. A. Brizzolara, N. A. Burnham, D. P. DiLella, K. P. Lee, C. R. K. Marrian, and R. J. Colton, J. Vac. Sci. Technol. A **8**, 3570 (1990).

[8] P. W. Tasker, J. Phys. C **12**, 4997 (1979).

[9] P. W. Murray, N. G. Condon, and G. Thornton, Phys. Rev. B **51**, 10 989 (1995).

[10] D. W. Bullett, J. Phys. C **16**, 2197 (1983).

[11] R. Wiesendanger, *Scanning Probe Microscopy* (Cambridge University Press, Cambridge, 1994).

[12] The choice of barrier height is somewhat difficult. A value of 1.6 eV was measured for $Na_{0.85}WO_3(001)$ [G. S. Rohrer, W. Lu, M. L. Norton, M. L. Blake, and G. S. Rohrer, J. Solid State Chem. **109**, 359 (1994)], but the work function for WO_3 is higher than for the metallic sodium tungsten bronzes (M. D. Hill, Ph.D. thesis, Oxford, 1984), suggesting a small upward adjustment of the barrier height.

[13] J. B. Pethica, J. Knall, and J. H. Wilson, in *Microscopy of Semiconducting Materials*, edited by A. G. Cullis *et al.*, IOP Conf. Proc. No. 134 (Institute of Physics, London, 1993).

[14] R. D. Bringans, H. Höchst, and H. R. Shanks, Vacuum **31**, 473 (1981).

[15] R. D. Bringans, H. Höchst, and H. R. Shanks, Surf. Sci. **111**, 80 (1981).

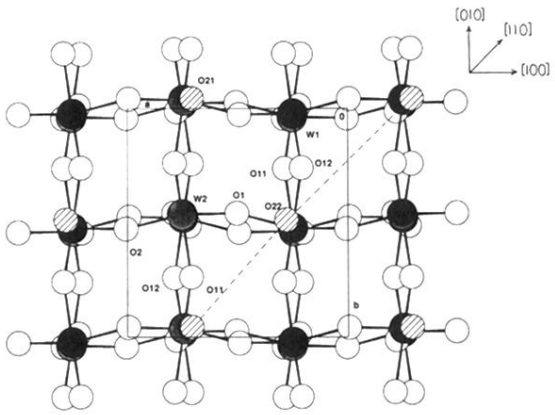

FIG. 1. Projection of the structure of monoclinic WO_3 onto the (001) plane. The surface is terminated with O ions (identified by hatching in the figure) above half the tungsten ions to give a $(\sqrt{2}\times\sqrt{2})R45°$ superstructure based on the primitive ReO_3-like cell. The dashed lines are added to emphasize alternately long and short O-O separations along the [110] direction.

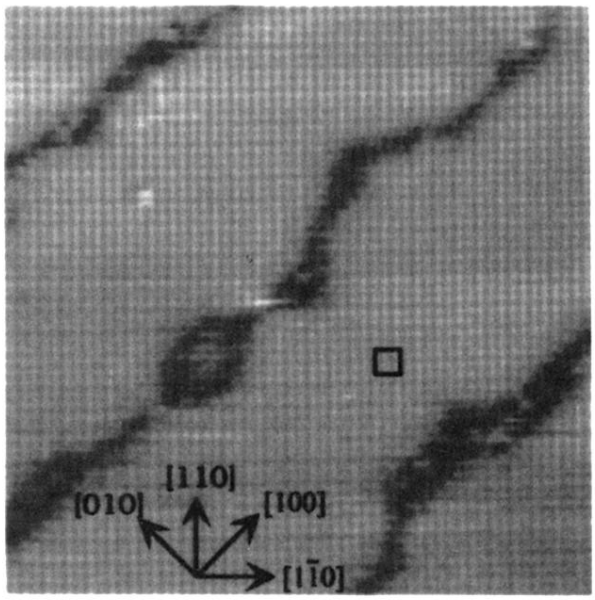

FIG. 2. 150 Å×150 Å image of WO_3(001) acquired at +1.5 V sample bias and a 1-nA tunnel current. The gray scale extends over 4.7 Å. The corrugation along the atomic rows in the [100] direction is 0.3 Å, while the dark troughs have a depth of 1.7 Å. The idealized $(\sqrt{2}\times\sqrt{2})R45°$ unit cell is shown in the figure.

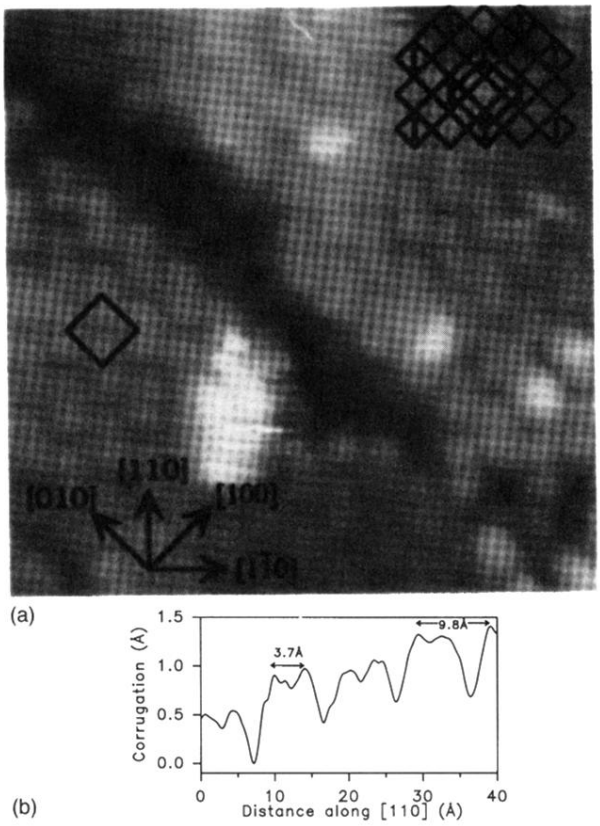

FIG. 3. (a) Higher resolution 78 Å$\times$78 Å image of $WO_3(001)$ acquired at $+2.0$ V sample bias and a 1-nA tunnel current. The gray scale extends over 5 Å. Note "dimerization" of topographic maxima along the [110] direction. The 2×2 supercell is highlighted in the figure and a schematic representation of the image is shown in the top right-hand corner of the figure. (b) Corrugation profile along the [110] direction. The periodicity of 9.8 Å along this direction introduced by dimerization of the topographic maxima corresponds roughly to $2\sqrt{2}\times3.7$ Å$=10.5$ Å within the error limits of the piezo calibration. Dimerization of topographic maxima is apparent.